

Battery aging and the Kinetic Battery Model

Marijn Jongerden and Boudewijn Haverkort

Design and Analysis of Communication Systems, University of Twente

Abstract

Batteries are omnipresent, and with the uprise of the electrical vehicles will their use will grow even more. However, the batteries can deliver their required power for a limited time span. They slowly degrade with every charge-discharge cycle. This degradation needs to be taken into account when considering the battery in long lasting applications. Some detailed battery models that describe the degradation exist. However, these are complex models that require detailed knowledge. These models are in general computationally intensive, which does not make them well suited to be used in a wider context. A model better suited for this is the Kinetic Battery Model. In this paper, we this model would change due to battery degradation, by the results of our experimental degradation analysis. In our analysis we see that the degradation takes place in two phases. After the first phase of slow degradation, the battery suddenly starts to degrade rapidly.

Keywords: battery modeling, battery measurement, battery degradation

1. Introduction

Batteries-powered devices are everywhere; smart-phones, laptops, wireless sensors, electric cars and many more. The batteries provide portable power to these devices. However, the batteries have a limited life span. Obviously non-rechargeable batteries can be discharged only once before they need to be replaced. But, even rechargeable batteries will not be usable after some time.

How long a battery can be used depends on many factors, such as battery type, discharge and charge current, depth of discharge and temperature. It is hard to predict the lifetime of a battery for any given workload pattern. Electro-chemical and electrical circuit models, that require detailed knowledge of the used batteries, are available in literature, see for example [1, 2]. In recent work, Wognsen et al. [3] propose an approach to compare the impact workload patterns have on the battery life through the Fourier Transform of the workload.

Although some theoretical work exists, little practical work is available in the scientific literature on measuring the battery degradation over time. In this report we present the results of our measurements on battery cells used in nano-satellite batteries.

These results are analyzed in the context of a widely used battery model, the Kinetic Battery Model. The analysis gives insight on how the degradation of the battery impacts the model parameters, and on how to possibly extend this model to cope with the effects of degradation.

20 The rest of this report is structured as follows. Section 2 gives a brief overview of related
21 work on battery degradation modeling. Section 3 introduces the Kinetic Battery Model. In
22 Section 4 the experimental set-up and the performed experiments are described. The results
23 of the experiments are given in Section 5. We end with a discussion of the results in Section
24 6.

25 **2. Related work**

26 There are several types of battery models available in the scientific literature. [4] provides
27 an overview of the most used models, such as electro-chemical models, electrical circuit
28 models and analytical models. In [4] the focus is on predicting the duration of a single
29 discharge cycle. These types of models are also used to describe the long term effects of
30 battery degradation.

31 In [1], capacity fading is modeled with a electro-chemical battery model of a lithium ion
32 battery. This type of model requires a very detailed knowledge of the battery, and are in
33 general very computationally intensive.

34 In [2] an electrical circuit model is made that models capacity fading due to cycling, as
35 well as the increase of the internal resistance due to cycling. The model should be configured
36 with data from the battery data sheets. However, as also the authors mention, in general,
37 it is very hard to obtain all required information.

38 High level analytical models, such as the the Kinetic Battery Model (KiBaM) [5], require
39 much less knowledge of the battery, and can be easily combined with other models. For
40 example, in [6] the KiBaM is extended to a random KiBaM and combined with a Markov
41 Task Process that models the battery load. With the combined model, one can compute
42 the probability the battery is depleted due to the defined load pattern. The KiBaM does
43 not take into account the how the battery degrades; it is not known how the parameters are
44 effected.

45 In this paper, we investigate the how the KiBaM-parameters change when the battery is
46 repeatedly discharged. We take an experimental approach. We wear the battery by applying
47 a relatively heavy load to the battery. This gives us the practical insight in how the battery
48 degrades over time.

49 **3. KiBaM theory**

50 The Kinetic battery model is a compact battery model that includes the most important
51 features of the battery, like the rate-capacity effect and recovery effect. The model has been
52 developed by Manwell and McGowan in 1993 [5]. Originally, the model was aimed at lead-
53 acid batteries, but analysis has shown it could also be used in battery discharge modeling
54 for other battery types [7].

In the model, the battery charge is distributed over two wells: the *available-charge* well
and the *bound-charge* well (cf. Figure 1). A fraction c of the total capacity is put in the
available-charge well (denoted $y_1(t)$), and a fraction $1 - c$ in the bound-charge well (denoted
 $y_2(t)$). The available-charge well supplies electrons directly to the load ($i(t)$), whereas the

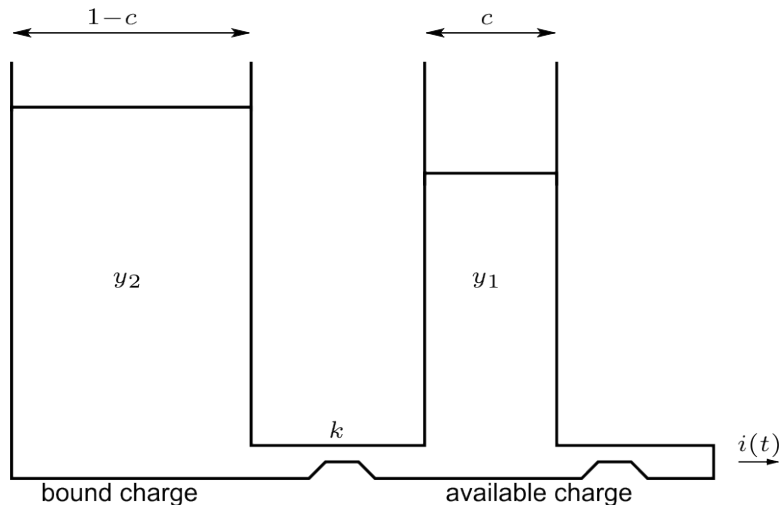


Figure 1: The two well model of the Kinetic Battery Model.

bound-charge well supplies electrons only to the available-charge well. The charge flows from the bound-charge well to the available-charge well through a “valve” with fixed conductance, k . The parameter k has the dimension 1/time and limits the rate at which the charge can flow between the two charge wells. Next to this parameter, the rate at which charge flows between the wells depends on the height difference between the two wells. The heights of the two wells are given by: $h_1(t) = y_1(t)/c$ and $h_2(t) = y_2(t)/(1-c)$. The change of the charge in both wells is given by the following system of differential equations:

$$\begin{cases} \frac{dy_1}{dt} = -i(t) + k(h_2 - h_1), \\ \frac{dy_2}{dt} = -k(h_2 - h_1), \end{cases} \quad (1)$$

55 with initial conditions $y_1(0) = c \cdot C$ and $y_2(0) = (1-c) \cdot C$, where C is the total battery
 56 capacity. The battery is considered empty when it is observed that there is no charge left
 57 in the available-charge well.

As shown in [7], we can transform the equations to

$$\begin{cases} \frac{d\gamma}{dt} = -i(t), \\ \frac{d\delta}{dt} = \frac{i(t)}{c} - k'\delta, \end{cases} \quad (2)$$

58 where $k' = k/(c(1-c))$, $\gamma = y_1 + y_2$ and $\delta = y_2/(1-c) - y_1/c$. We can interpret γ as the
 59 total charge remaining in the battery, and δ as the height difference between the the charge
 60 levels of the two wells. The initial conditions transform into $\gamma(0) = C$ and $\delta(0) = 0$. The
 61 battery is empty when $\gamma(t) = (1-c)\delta(t)$.

62 *3.1. KiBaM constant current discharge*

When we consider a constant current discharge, i.e., $i(t) = I_d$, the differential equations are easily solved. The solution is:

$$\begin{cases} \gamma(t) = C - I_d t, \\ \delta(t) = \frac{I_d}{ck'} (1 - e^{-k't}). \end{cases} \quad (3)$$

The battery lifetime L , i.e., the time to empty the available charge well, for a constant current discharge is given by:

$$L = \frac{C}{I_d} - \frac{1}{k'} \left(\frac{1-c}{c} + W \left(\frac{1-c}{c} e^{\frac{1-c}{c} - \frac{ck'}{I_d}} \right) \right), \quad (4)$$

63 where $W(\cdot)$ is the so-called Lambert W function [8]. The Lambert W function is the inverse
64 function of $f(x) = xe^x$.

65 By measuring the the battery lifetime, and the delivered energy, as a function of the
66 discharge current, we can determine the KiBaM parameters, k , c and C by fitting Equation
67 4 to the data.

68 *3.2. KiBaM charging*

69 Battery charging normally is performed in two phases. First, the battery is charged
70 at a constant current. In this phase the voltage slowly rises. When the voltage reaches
71 the maximum level, V_{max} , the second phase starts. During this phase the voltage is kept
72 constant at V_{max} , and the charging current will drop.

73 We discuss the two charging phases in the context of the KiBaM model in the following
74 sections.

75 *3.2.1. KiBaM constant current charging*

In the KiBaM, the charging with a constant current is very similar to discharging with
a constant current. For a constant charging current I_{ch} the KiBaM equations are:

$$\begin{cases} \frac{dy_1}{dt} = I_{ch} - k \left(\frac{y_1}{c} - \frac{y_2}{1-c} \right), \\ \frac{dy_2}{dt} = k \left(\frac{y_1}{c} - \frac{y_2}{1-c} \right). \end{cases} \quad (5)$$

When we consider the battery fully empty at the start of the charging, the initial conditions
are $y_1(0) = 0$ and $y_2(0) = 0$. The constant current charging phase ends when the available
charge well is filled, thus $y_1 = cC$. In terms of $\delta_{ch} = \frac{y_1}{c} - \frac{y_2}{1-c}$ ($\delta_{ch} = -\delta$) and $\gamma = y_1 + y_2$,
the equations are:

$$\begin{cases} \frac{d\gamma}{dt} = I_{ch}, \\ \frac{d\delta_{ch}}{dt} = \frac{I_{ch}}{c} - k'\delta_{ch}, \end{cases} \quad (6)$$

76 The initial conditions transform into $\delta_{ch}(0) = 0$ and $\gamma(0) = 0$. The condition for the end of
77 the constant current charging phase is $\gamma(t_{lin}) + (1 - c)\delta_{ch}(t_{lin}) = C$. This condition can be
78 interpreted as follows, at time $t = t_{lin}$, the amount of energy put into the battery is $\gamma(t_{lin})$
79 and still $(1 - c)\delta_{ch}(t_{lin})$ needs to be charged.

The solutions for γ and δ_{ch} are again easily obtained:

$$\begin{cases} \gamma(t) &= I_{ch}t, \\ \delta_{ch}(t) &= \frac{I_{ch}}{ck'}(1 - e^{-k't}), \end{cases} \quad (7)$$

80 where we see that the equation for δ is the same as for discharging, cf. (3).

Under the described conditions, the time it takes to fill the available charge well, t_{lin} , is the similar to the discharging lifetime, cf. (4):

$$t_{lin} = \frac{C}{I_{ch}} - \frac{1}{k'} \left(\frac{1 - c}{c} + W \left(\frac{1 - c}{c} e^{\frac{1-c}{c} - \frac{ck'}{I_{ch}}} \right) \right). \quad (8)$$

81 So, under the assumption that the battery is completely empty, we expect that, when the
82 battery parameters are the same for charging an the linear charging phase takes as long as
83 the discharging lifetime.

84 3.2.2. KiBaM non-linear charging

85 After the linear charging phase, the battery is charged with a constant voltage and a
86 decreasing current. In the KiBaM we can interpret this as follows. The constant voltage
87 keeps the level of the available charge well at its maximum. The rate at which the battery
88 can accept additional charge is limited by the flow between the two charge wells. This rate
89 depends on the height difference between the two wells, and thus will decrease when the
90 battery is further charged.

The available charge does not change, hence, $\frac{dy_1}{dt} = 0$. From the KiBaM equations we obtain:

$$i(t) = k \left(\frac{y_1}{c} - \frac{y_2}{1 - c} \right). \quad (9)$$

In terms of $\delta_{ch} = \frac{y_1}{c} - \frac{y_2}{1 - c}$ this yields:

$$i(t) = k\delta_{ch} = k'c(1 - c)\delta_{ch} \quad (10)$$

The KiBaM equations in terms of δ_{ch} and γ now are,

$$\begin{cases} \frac{d\gamma}{dt} &= i(t) = k'c(1 - c)\delta_{ch}, \\ \frac{d\delta_{ch}}{dt} &= \frac{i(t)}{c} - k'\delta_{ch} = -k'c\delta_{ch}, \end{cases} \quad (11)$$

From these equations it follows that

$$\delta = \delta_0 e^{-ck't}, \quad (12)$$

Table 1: Parameters of the GomSpace batteries [9]

name	value
nominal capacity	2600 mAh
maximum charge voltage	4.2 V
end of discharge voltage	3.0 V
maximum discharge current	3.75 A
maximum charge current	2.5 A
end of charge current	1.3 A
charge temperature range	-5 — 45 °C
discharge temperature range	-20 — 60 °C

91 where δ_0 is the height difference between the two wells at the start of the non-linear charging
 92 phase (I_{lin}). δ_0 depends on the charging current in the linear phase. From equations (7) and
 93 (8) it follows that

$$\delta_0 = \frac{I_{lin}}{ck'} \left(1 - e^{-ck't_{lin}}\right). \quad (13)$$

94 If $k't_{lin}$ is large, that is, if the height difference has approached its maximum value during
 95 the linear charging phase, we obtain

$$\delta_0 = \frac{I_{lin}}{ck'}. \quad (14)$$

96 The height difference decreases exponentially, and thus the charging current should de-
 97 crease exponentially. By fitting an exponential function to the measured current we can
 98 estimate the factor ck' . This gives additional information on how the KiBaM performs for
 99 charging the battery.

100 4. Experimental set-up

101 In the experiments we analyze 4 Li-ion battery cells with a capacity of 2600 mAh,
 102 obtained from GomSpace. The nano satellite battery packs consist of 4 to 8 of these battery
 103 cells. Table 1 gives an overview of the key parameters, as provided in the datasheets.

104 The measurements are done with the Cadex C8000 battery testing system. The tester
 105 is programmed to discharge and charge the cells in a controlled fashion according to a user-
 106 defined load profile, while measuring the voltage, current and temperature. This data is
 107 logged each second, and is used for the analysis of the battery properties. The system has
 108 four connections to test four batteries simultaneously. Figure 2 shows the set-up with the
 109 batteries and the Cadex system.

110 The experiments consist of multiple phases. In the first phase, *KiBaM estimation mea-*
 111 *surements*, the cells are discharged and charged at various constant rates. The charge rates
 112 vary from 0.1C to 0.9C, while the discharge rates vary from 0.1C to 1.4C. Table 2 gives
 113 an overview of the discharge and charge currents of the individual measurement cycles.

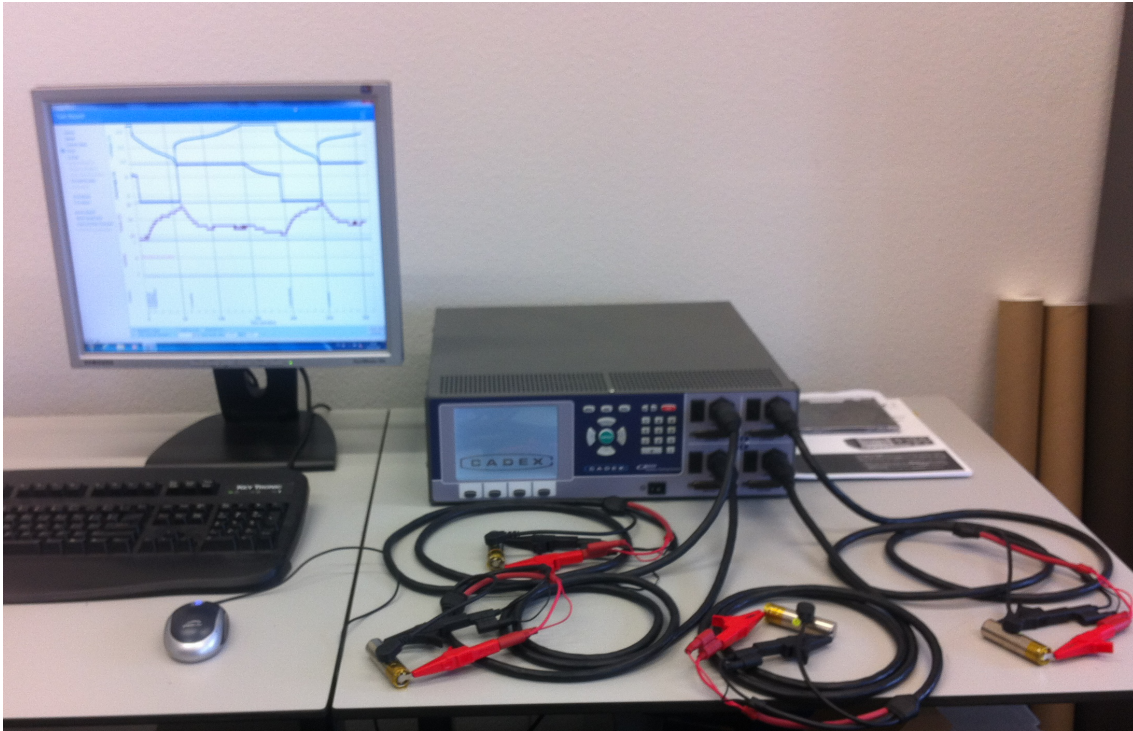


Figure 2: Experimental set-up with the Cadex C8000 battery tester.

Table 2: Discharge and charge currents for the KiBaM parameter estimation measurements.

test	discharge current	charge current
1	0.1C = 0.26 A	0.1C = 0.26 A
2	0.2C = 0.52 A	0.2C = 0.52 A
3	0.3C = 0.78 A	0.3C = 0.78 A
4	0.4C = 1.04 A	0.4C = 1.04 A
5	0.5C = 1.3 A	0.5C = 1.3 A
6	0.6C = 1.56 A	0.6C = 1.56 A
7	0.7C = 1.82 A	0.7C = 1.82 A
8	0.8C = 2.08 A	0.8C = 2.08 A
9	0.9C = 2.34 A	0.9C = 2.34 A
10	1.0C = 2.60 A	0.6C = 1.56 A
11	1.2C = 2.86 A	0.7C = 1.82 A
12	1.4C = 3.64 A	0.9C = 2.34 A

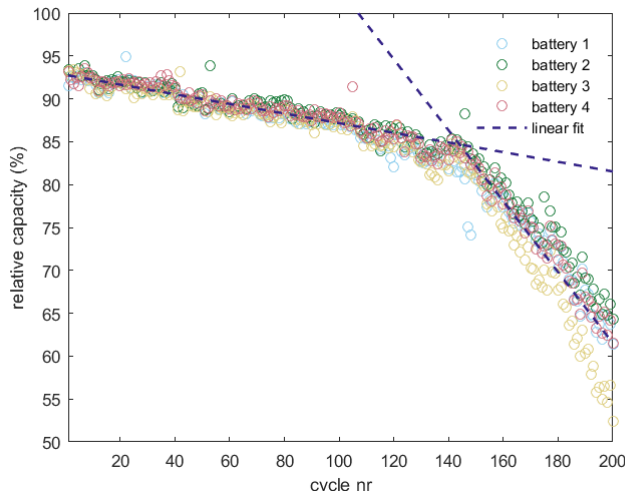


Figure 3: Capacity relative to the nominal capacity as a function of the cycle number.

114 The data from these measurements will be used to estimate the parameters for the Kinetic
 115 Battery Model.

116 In the second phase, *the degradation measurements*, the cells are repeatedly fully dis-
 117 charged at 1C and charged at 0.5C. This high load will result in a relative fast degradation
 118 of the cells. After 50 discharge-charge cycles, the cycles of the first phase are repeated, in
 119 order to see whether and how the battery parameters have changed. The measurements of
 120 50 discharge-charge cycles, and determining the battery parameters will be repeated until
 121 the cell capacity has dropped below 80% of its initial value. The results of these experiments
 122 give an indication on how the cells degrade over time.

123 5. Results

124 In this section we discuss the results of the performed measurements. First, we analyze
 125 the battery degradation due to the degradation measurements in Section 5.1. Then, we
 126 analyze the change of the KiBaM parameters for discharging and charging in Sections 5.2
 127 and 5.3, respectively.

128 5.1. Degradation measurements

129 Figure 3 shows how the discharge capacity decreases as a function of the discharge cycle
 130 number. In the first discharge cycle, on average, the batteries deliver 92.8% of the nominal
 131 capacity (2600 Ah). In the subsequent cycles the discharge capacity slowly drops. The
 132 decrease in capacity is more or less linear. We fit a linear function, $y = \alpha \cdot \text{cycle} + \beta$
 133 to the first 100 measurements. The fit yields $\alpha = -0.057 \pm 0.0025$ and $\beta = 92.8 \pm 0.14$. This
 134 means that the capacity, on average, drops 0.057 percentage point with every discharge-
 135 charge cycle.

136 After approximately 140 cycles the capacity decreases more rapidly. Battery 3 now
 137 degrades clearly faster than the other 3 batteries. We fit another line, $\text{Cap} = \alpha \cdot \text{cycle} + \beta$,

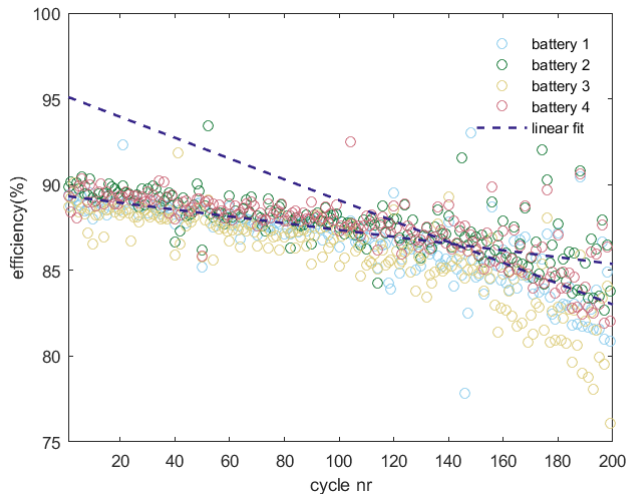


Figure 4: Efficiency of charge discharge cycle as a function of the cycle number.

138 to the last 50 measurements, cycle 151 to 200. This yields, $\alpha = -0.41 \pm 0.027$ and $\beta =$
 139 144.2 ± 4.8 . This means that the degradation is more than a factor 7 faster than at the
 140 start, with an average of 0.41 percent point per cycle.

141 Next to the capacity we investigate how the efficiency evolves when the battery is used.
 142 The efficiency is determined by: $E_{dis,n}/E_{ch,n-1}$, where $E_{dis,n} * 100$ is the delivered energy in
 143 cycle n , and $E_{ch,n-1}$ is the charging energy of cycle $n - 1$.

144 The results are shown in Figure 4. As for the capacity, we see that the efficiency also
 145 degrades in two phases. Again we fit two lines to the data. The first line is fit to the first
 146 100 cycles. The efficiency starts at $89.3\% \pm 0.17$. The efficiency degrades linearly with a rate
 147 of 0.020 ± 0.0028 percent point per cycle.

148 The second line is fit to the last 50 cycles. Here we see that the efficiency degrades at
 149 a rate of 0.061 ± 0.022 percent point per cycle. This means that the efficiency degrades 3
 150 times faster at the end of the battery life than at the beginning. Furthermore, we see that
 151 the variance in efficiency is much larger at the end of the battery lifetime.

152 Finally, we investigate the non-linear charge phase of the degradation measurements.
 153 According to the KiBaM theory the charge current should drop exponentially during the
 154 non-linear charge phase, cf. (12). We fit a negative exponential curve to the measured
 155 current. In Figure 5 the exponent, which corresponds to $k'c$, is plotted as a function of
 156 the cycle number. We see that the exponent decreases as the number of discharge-charge
 157 cycles increases. We have fitted a linear curve, $y = \alpha \cdot x + \beta$ to the data. This fit yields
 158 $\alpha = -1.71 \cdot 10^{-6} \pm 0.05 \cdot 10^{-6}$ and $\beta = 1.03 \cdot 10^{-3} \pm 0.005 \cdot 10^{-3}$. In the KiBaM, the decrease
 159 of the exponent $k'c$ is either caused by a decrease in k , i.e., the conductance between the
 160 available and bound charge well, or by a decrease in c , i.e., the size of the available charge
 161 well.

162 However, the KiBaM does not include the efficiency of the charging process. As we have
 163 seen earlier, the efficiency of the battery drops as the battery ages. This drop in efficiency

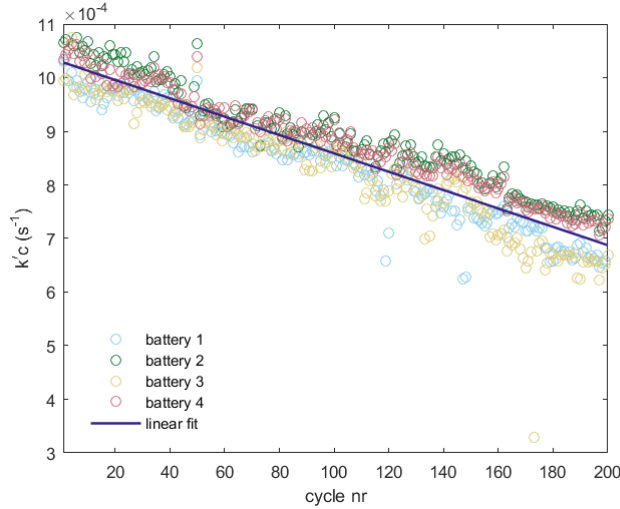


Figure 5: The exponent for the non-linear charge phase as a function of the cycle number.

164 can also result in the slower exponential drop of the charging current during the non-linear
 165 charging phase.

166 5.2. Discharge KiBaM parameter estimation

167 We start the battery degradation analysis with a series of measurements for determining
 168 the KiBaM parameters. In these measurements the batteries are discharged and charged
 169 at various constant currents, cf. Table 2. These measurements have been repeated after
 170 every 50 cycles in the degradation measurements. Figure 6(a) shows the measured discharge
 171 capacity of the four batteries for the different discharge currents of the first series.

172 The measurements at $0.9C = 2.34$ A discharging current have been performed twice. The
 173 first run, which was the first experiment that was performed, resulted for all batteries in a
 174 discharge capacity that was higher than expected. The second run resulted in a capacity
 175 that was in line with the other experiments. The reason for these results remains unclear.

176 For battery 3, we see a relative low capacity at the low discharge currents. We expect
 177 that this is some internal damage or lower quality of the battery. Battery 3 has a slightly
 178 lower performance throughout the experiments, as we will see in the later results.

The measured delivered capacity (C_{del}) in As as a function of the discharge current (I_d)
 is fitted to the function (cf. 4):

$$C_{del} = C_{nom} - \frac{I_d}{k'} \left(\frac{1-c}{c} + W \left(\frac{1-c}{c} e^{\frac{1-c}{c} - \frac{C_{nom} k'}{I_d}} \right) \right) \quad (15)$$

179 In the fitting procedure we use the parameter $\kappa = 1/k'$ instead of k' , since the fitting
 180 algorithm was not stable when k was used directly. In the fit we ignored the outliers of the
 181 first measurement and battery 3. The result is included in Figure 6(a). From the fit we
 182 obtained $C = 9.67 \cdot 10^3$ As ± 220 As, which is higher than the nominal capacity of 2600 mAh
 183 = 9360 As. The other parameters are: $c = 0.90 \pm 0.015$ and $\kappa = 9.36 \cdot 10^3$ s $\pm 9.12 \cdot 10^3$ s. The

Table 3: parameters discharge

experiment	$C(10^3 \text{ As})$	c	$\kappa (10^3 \text{ s})$
series 1	9.67 ± 0.22	0.90 ± 0.015	9.36 ± 9.12
series 2	9.25 ± 0.10	0.90 ± 0.019	4.37 ± 2.66
series 3	9.23 ± 0.08	0.86 ± 0.019	3.76 ± 1.56
series 4	9.26 ± 0.15	0.83 ± 0.027	4.43 ± 2.24
series 5	8.67 ± 0.26	0.70 ± 0.080	2.85 ± 2.05

parameter κ has a very large confidence interval, thus we cannot draw any strong conclusions on the actual value of this parameter, or the parameter $k = 1/\kappa$.

After every 50 discharge-charge cycles another series of measurements is done to determine the KiBaM parameters. The results are given in Figures 6(b) - 6(e). In these figures we see that, like in the degradation measurements, the capacity first drops slowly in Figures 6(b) to 6(d), and then drops dramatically in Figure 6(e). In all these measurement series, as in the results of the first series, battery 3 has a lower capacity for the low discharge currents. At high discharge currents, greater than 2.5 A, all batteries perform less than expected. When we include these measurements in the fitting procedure the results for the parameters c and κ are nearly meaningless, with extremely large confidence intervals. The degradation of the battery seems to have a larger impact when high discharge currents are applied.

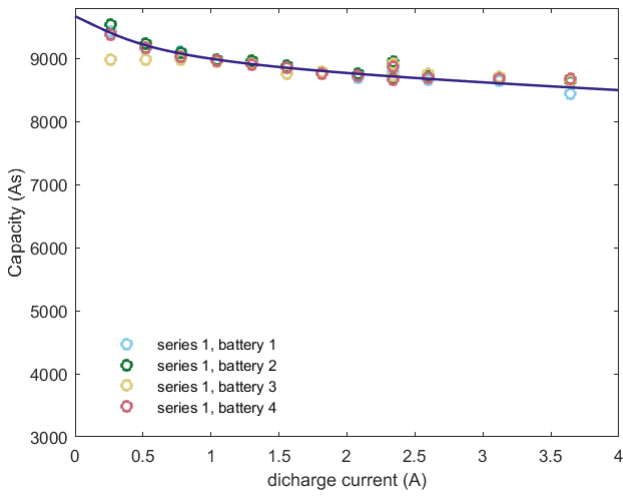
When we discard the high current measurements in the fitting procedure, the results are more in line with the analysis of the first measurement series. The values of the fitted parameters and their confidence intervals are given in Table 3. We see a decrease in the capacity of the battery, as expected. Also, the parameter c slowly decreases, as the battery ages. This means that the decrease in capacity affects the available more than the bound charge. For the parameter κ it is impossible to tell whether the battery degradation has any real impact, due to the large confidence intervals.

5.3. KiBaM charging

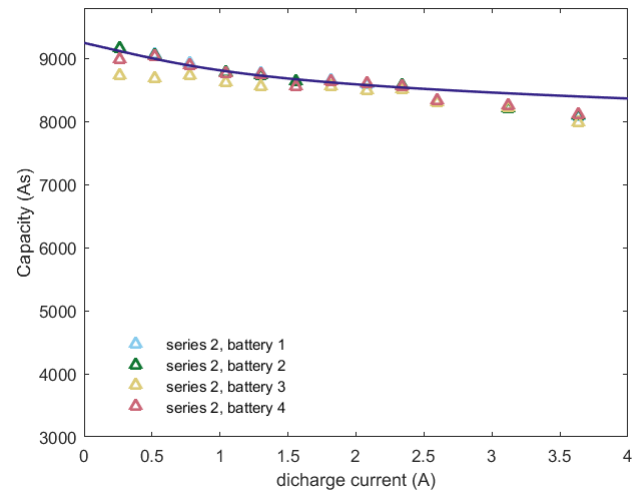
Next to the KiBaM parameters for discharging, we fit the KiBaM to the charging measurements. Figure 7 shows the energy put into the battery during the linear charge phase of the five series. In all five figures we notice some deviating measurements. These measurements coincide with the deviations in the discharge results. Battery 3, again deviates at low currents. However, the linear charge capacity is larger than for the other batteries at low currents, whereas the discharge capacity was lower.

The outliers are again discarded in the fitting procedure. The fitted curves are given in Figure 7, and the parameters are given in 4. Again, we can see that the capacity decreases. The estimated capacity is, however, smaller than for discharging. The parameter c is much smaller during charging than during discharging. This implies that the available charge well is much smaller when the battery is charged.

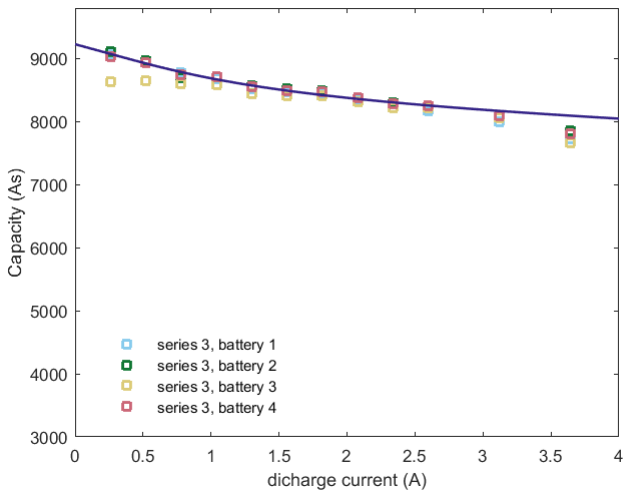
For the parameter κ it is again hard to draw firm conclusions. The estimated values for κ are lower for charging than for discharging. This would suggest that the flow between bound and available charge is faster during charging than during discharging.



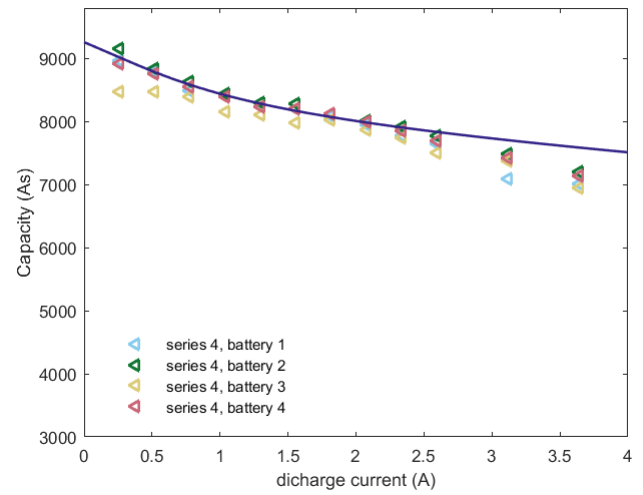
(a) series 1



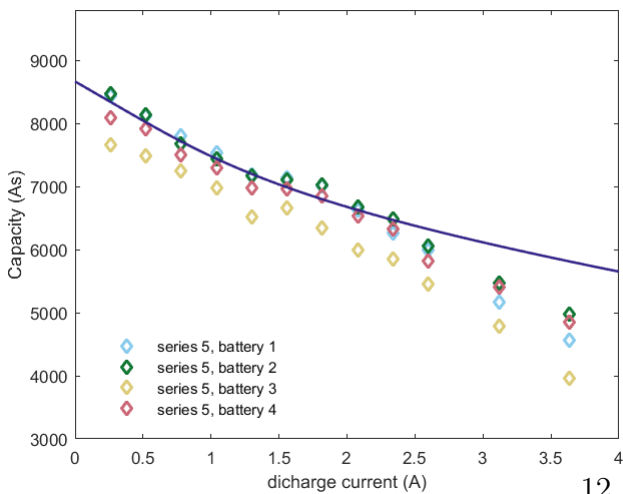
(b) series 2



(c) series 3



(d) series 4



(e) series 5

Figure 6: KiBaM discharge fits

Table 4: parameters charge

experiment	$C(10^3 \text{ As})$	c	$\kappa (10^3\text{s})$
series 1	9.38 ± 0.12	0.579 ± 0.076	1.74 ± 0.73
series 2	9.22 ± 0.09	0.646 ± 0.031	2.57 ± 0.59
series 3	9.18 ± 0.12	0.599 ± 0.045	2.37 ± 0.70
series 4	9.09 ± 0.15	0.548 ± 0.057	2.22 ± 0.78
series 5	8.57 ± 0.27	0.504 ± 0.071	2.62 ± 1.21

217 It is not clear how to interpret the differences between the KiBaM parameters for dis-
 218 charging and charging within the context of the battery processes. However, this does show
 219 that when the KiBaM model is used, we cannot just reverse the flow of the current and keep
 220 the parameters the same when we switch from discharging to charging.

221 6. Discussion

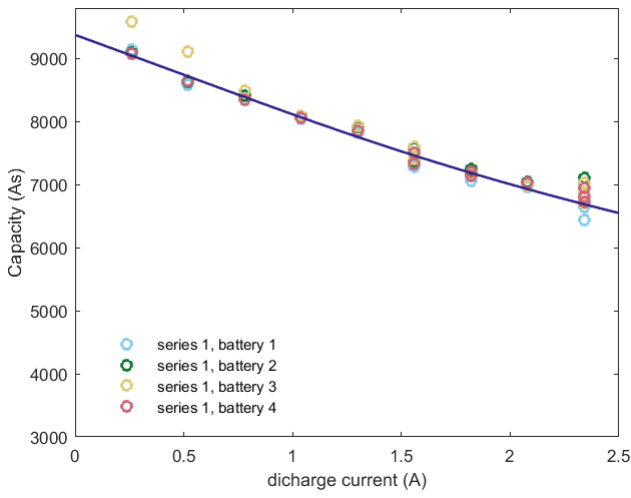
222 The degradation measurements clearly show the degradation of the battery during its
 223 cycle life. We see a linear drop in the capacity until approximately 140 cycles. After this
 224 point the capacity starts to degrade at a much higher rate. This point, 140 cycles, could
 225 be taken as the effective cycle life of the battery. Of course, we should add the 37 cycles
 226 of the KiBaM parameter estimation measurements to this to get a proper estimation of the
 227 cycle life of the batteries. This gives us a cycle life of approximately 180 cycles. This is
 228 much lower than the 350 cycles at 1C discharge rate that are given in the data sheets. This
 229 difference might be caused by temperature effects During the discharge periods the batter
 230 temperature typically rose to 34°C, while dropping to 25°C during charging. Whereas the
 231 cycle life in the data sheet assumes a constant temperature of 25°C.

232 Next to the capacity loss, we see a decrease in the efficiency of the battery. The efficiency
 233 drops from approximately 90% at the start of the experiments to approximately 86% at the
 234 end of the cycle life of the batteries. We do not see a change in the rate at which the efficiency
 235 decreases after the cycle life has been reached.

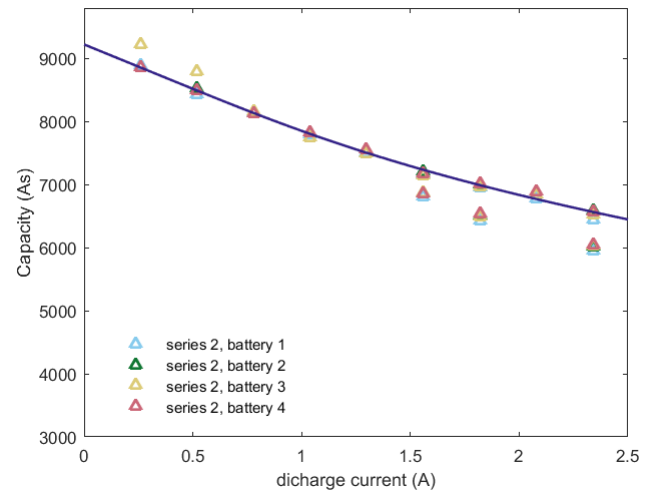
236 The analysis of the non-linear charge phase shows us that the exponential decay of the
 237 charging current becomes slower as the battery ages. Although this might indicate a change
 238 in the KiBaM parameters c and k , this also might be caused by the decreasing efficiency.

239 The measurements for estimating the KiBaM parameters as well show the drop in the
 240 capacity for the aging battery. The fraction of available charge, parameter c , shows a
 241 decrease as well in the discharging measurements. In the charging measurements this decay
 242 is not so clear. However we do see that the parameter c is different for discharging and
 243 charging. The analysis gives no conclusive results for how the parameter k evolves for the
 244 aging batteries.

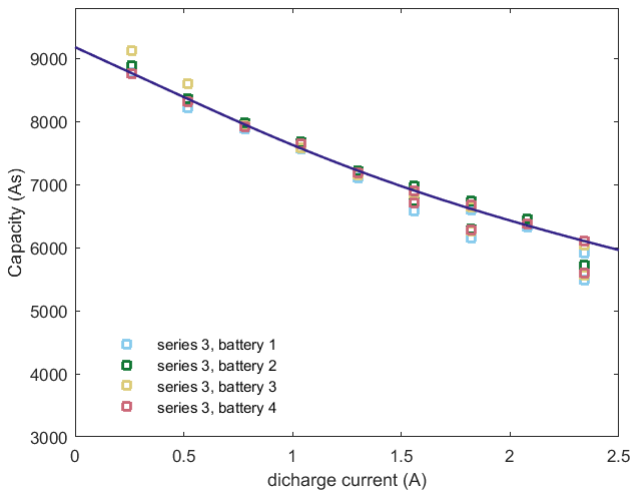
245 The experiments put forward a couple of limitations of the KiBaM. Although the decay
 246 of the capacity and the drop of the efficiency of the battery might be easily included into a
 247 more evolved KiBaM, the asymmetry between discharging and charging in the parameter c
 248 may not be incorporated so easily. Changing c when the battery changes from discharging



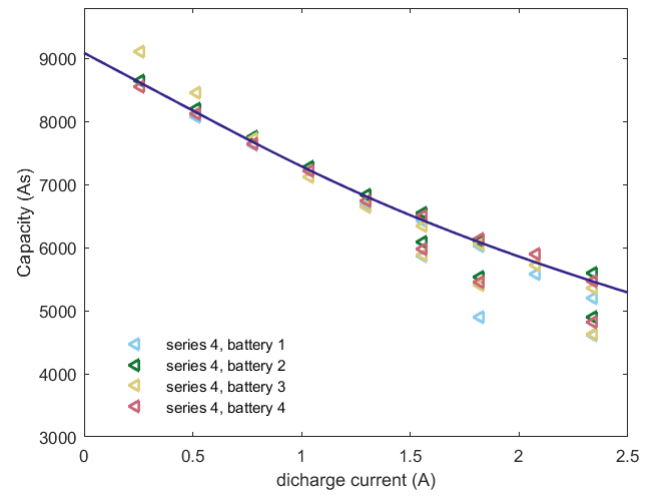
(a) series 1



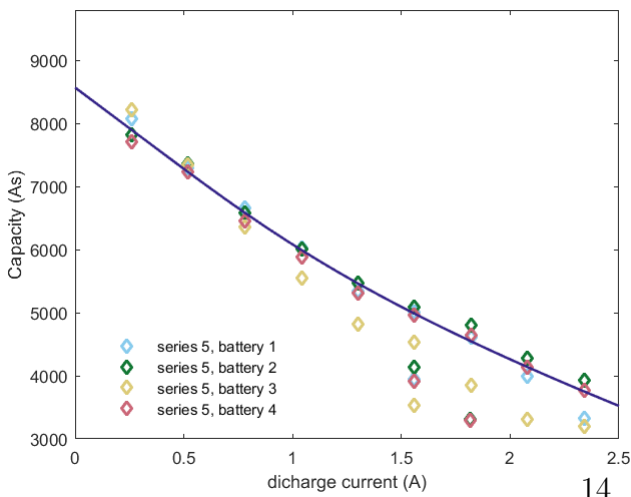
(b) series 2



(c) series 3



(d) series 4



(e) series 5

Figure 7: KiBaM charge fits

249 to charging, might involve a redistribution of the available and bound charge as well. More
250 analysis, and possibly more measurements, are needed to see how we should adapt the
251 KiBaM to incorporate the observed phenomena.

252 references

- 253 [1] G. Ning and B. N. Popov, "Cycle life modeling of lithium-ion batteries," *Journal of The Electrochemical*
254 *Society*, vol. 151, no. 10, pp. A1584–A1591, 2004.
- 255 [2] M. Petricca, D. Shin, A. Bocca, A. Macii, E. Macii, and M. Poncino, "Automated generation of battery
256 aging models from datasheets," in *Proceedings of the 32nd IEEE International Conference on Computer*
257 *Design (ICCD)*, pp. 483–488, IEEE, 2014.
- 258 [3] E. R. Wognsen, B. R. Haverkort, M. Jongerden, R. R. Hansen, and K. G. Larsen.
- 259 [4] M. R. Jongerden and B. R. Haverkort, "Which battery model to use?," *IET Software*, vol. 3, no. 6,
260 pp. 445–457, 2009.
- 261 [5] J. F. Manwell and J. G. McGowan, "Lead acid battery storage model for hybrid energy systems," *Solar*
262 *Energy*, vol. 50, no. 5, pp. 399–405, 1993.
- 263 [6] H. Hermanns, J. Krčál, and G. Nies, "Recharging probably keeps batteries alive," in *International*
264 *Workshop on Design, Modeling, and Evaluation of Cyber Physical Systems*, pp. 83–98, Springer, 2015.
- 265 [7] M. R. Jongerden, *Model-based energy analysis of battery powered systems*. PhD thesis, University of
266 Twente, Enschede, December 2010.
- 267 [8] Wolfram Mathworld, Lambert-W Function, "[http://mathworld.wolfram.com/LambertW-](http://mathworld.wolfram.com/LambertW-Function.html)
268 [Function.html](http://mathworld.wolfram.com/LambertW-Function.html)," 2015. Accessed November 2016.
- 269 [9] GomSpace, "NanoPower Battery Datasheet, Lithium Ion 18650 cells for space flight products," 2012.
270 supplied by GomSpace, 2015.